МАТЕМАТИЧЕСКОЕ МОДЕЛИРОВАНИЕ

MSC 49N90 DOI: 10.14529/mmp260301

STOCHASTIC DYNAMICS OF OPTIMAL PANDEMIC CONTROL

E.A. Gubar[1]***, V.A. Taynitskiy***[1]***, I. Dahmouni***[2]
[1]St. Petersburg State University, St. Petersburg, Russian Federation
[2]University of British Columbia, Vancouver, Canada
E-mail: e.gubar@spbu.ru, tainitsky@gmail.com, ilyass.dahmouni@ubc.ca

We develop an evolutionary SIR model with a stochastic information layer to analyze how uncertainty affects infection dynamics at the onset of a pandemic. The framework incorporates two forms of uncertainty: (i) uncertainty in health indicators, including unknown initial infection rates, and (ii) uncertainty in the information-updating process arising from interactions between individuals exposed to competing information types. We characterize the stability properties of the stochastic system and compare the resulting evolutionary dynamics with those of the corresponding deterministic model. We then formulate and solve the associated optimal control problem, deriving the optimal trajectory of the planner's information-control effort. Numerical simulations illustrate how parameter variations influence infection dynamics and the optimal level of the social planner's intervention aimed at improving information reliability in the population.

Keywords: control system analysis; optimal control; sir model; epidemic process; misinformation spreading.

Introduction

The coronavirus pandemic (Covid-19) renewed debate on the adequacy of epidemiological modelling tools and the reliability of early-stage data [1, 2]. The first waves of a novel virus are typically characterized by severe informational deficiencies, uncertain estimates of key epidemiological indicators, and limited ability to monitor individual behaviour at scale. Consequently, early policy responses are often implemented under incomplete information.

Mobility restrictions became one of the most widely used policy instruments, but responses varied substantially across jurisdictions. The UK initially pursued a strategy oriented toward natural immunity, Sweden avoided strict mobility limitations, while France and Italy implemented containment measures rapidly. China adopted a far more stringent "zero-Covid" policy. Similar heterogeneity appeared within countries: in the United States, New York and California imposed restrictions, whereas Texas opted for minimal interventions; in Canada, Ontario adopted moderate restrictions, while Quebec implemented stricter measures, including nightly curfews. Despite these differences, all governments faced uncertainty regarding early infection levels and transmission rates.

Reliable forecasts of infection dynamics depend on data quality and modelling assumptions. In the US, for example, the Centers for Disease Control and Prevention (CDC) created the US COVID-19 Forecast Hub to synthesize probabilistic forecasts of cases, hospitalizations, and mortality across geographic units [3]. Such initiatives illustrate the central role of uncertainty in early-stage pandemic management.

Deterministic SIR-type models are widely used to study epidemic dynamics, but they usually assume known initial infection levels and do not fully account for uncertainty in behavioural responses or information diffusion [4–7]. Recent work has incorporated evolutionary dynamics and competing information types [8–10]; however, the literature has not yet systematically examined how uncertainty in both epidemiological indicators and information interactions affects epidemic dynamics or optimal intervention strategies [11]. This gap motivates the present study.

We focus on the initial phase of a pandemic and study how uncertainty affects coupled epidemiological and informational processes. The model combines four subsystems: (i) an evolutionary SIR framework with uncertainty over early infection levels and transmission indicators; (ii) information diffusion, where individuals are exposed to either accurate information or fake news [12] and update beliefs voluntarily or through government awareness campaigns; (iii) stochastic uncertainty in both health indicators and informational interactions; and (iv) an optimal control problem in which a benevolent regulator seeks to reduce infections and misinformation under a budget constraint by minimizing the costs of infections, awareness campaigns, and immunisation. Together, these components generate a coupled stochastic system whose behaviour we analyse in detail.

The paper makes four contributions. First, it extends the deterministic evolutionary SIR-information model of [8] to a stochastic framework incorporating uncertainty in both epidemiological indicators and information interactions. Second, it characterizes the stability properties of the resulting stochastic system and shows how uncertainty modifies infection dynamics relative to the deterministic case. Third, it formulates and solves an optimal control problem in which the planner regulates information integrity under uncertainty, contributing to the literature on optimal control and pandemic management [13–18]. Fourth, it provides numerical simulations illustrating how parameter values and uncertainty intensity affect infection dynamics and the optimal control strategy.

The paper is organized as follows. Section 2 introduces the model parameters, transition structure, and payoff functions. Sections 2 and 3 analyse hidden and direct control. Section 4 derives the steady states and equilibrium properties. Section 5 presents numerical simulations, and Section 5concludes with results and possible extensions.

1. SIR Model

Extending [8], we use a system of nonlinear differential equations with an infinite time horizon to model the epidemic process. We denote by N the total number of nodes (individuals) in the network (society). Each individual is restricted to one of the three subgroups that constitute the pillars of the SIR model, i.e. *Susceptible*, *Infected* and *Recovered* so that at each instant of time we have $n_S(t) + n_I(t) + n_R(t) = N$. Let $S(t) = \frac{n_S(t)}{N}$, $I(t) = \frac{n_I(t)}{N}$, $R(t) = \frac{n_R(t)}{N}$ as fractions of *Susceptible*, *Infected* and *Recovered* nodes, respectively. We start by assuming that, at the outbreak of the pandemic, the majority of individuals are in the "Susceptible" category and that a relatively smaller (but unknown) proportion of individuals belong to the "Infected" subgroup. Let $\Gamma = \{S; I; R\}$, the initial conditions of the SIR model are then given by $S(0) = S^0_\phi > 0$, $I(0) = I^0_\phi > 0$, and $R(0) = R^0_\phi = 1 - S^0_\phi - I^0_\phi$. Where Γ^0_ϕ represents the expected initial state of the node $\Gamma = \{S; I; R\}$. Γ^0_ϕ can take two values, Γ^0_h with probability $p \in [0, 1]$ if the initial infection rate is high or Γ^0_l with probability $1 - p$ if the initial infection rate is low, that is $\Gamma^0_\phi = p\Gamma^0_h + (1 - p)\Gamma^0_l$.

Next, we introduce an evolutionary dynamic game into the model, in which individuals are of two types according to the information flow to which they belong: those who believe in "fake news" and those who are correctly warned, i.e. exposed to "real news". In line with the literature, we will refer to them by warned-fake (W_f) and warned-real (W_r), with $W_f + W_r = N$. The evolutionary game is based on the interaction of each individual (regardless of their beliefs) with the rest of society. At each moment, each player (individual) is subject to an update of their beliefs as a result of this exchange. However, we don't rule out the possibility that the outcome of the evolutionary game will lead individuals to hold to their original stance. The Government is not, however, positioned to evaluate the outcome of the interaction and therefore cannot provide precise estimates of the number of warned-false and warned-real individuals in each period. Once again we reiterate the role that the initial conditions play in our model, that is to influence the outcome of the evolutionary game.

The dynamic behaviour of the SIR model is provided by a system of nonlinear differential equations as follows:

$$dS_\phi/dt = -\beta_\phi S_\phi I_\phi;\ dI_\phi/dt = \beta_\phi S_\phi I_\phi - \sigma I_\phi;\ dR_\phi/dt = \sigma I_\phi, \tag{1}$$

where $\beta_\phi \in [0, 1]$ and $\sigma \in [0, 1]$ are the transition coefficients between the Susceptible to Infected, and Infected to Recovered subgroups respectively.

Fig. 1 outlines the process: the evolutionary game (red/green dots) transitions from S to I to R via two routes with probabilities p and $1 - p$, each corresponding to an infection level I_ϕ. Susceptible individuals may also jump directly to R by vaccination. At any time, independent of p, the population splits into real-news readers (x_r, green) and fake-news readers (x_f, red), with $x_f(t) + x_r(t) = 1$. Real-news individuals adopt protective measures (distancing, masking, early vaccination), while fake-news individuals behave inappropriately; thus, higher x_r reduces infections.

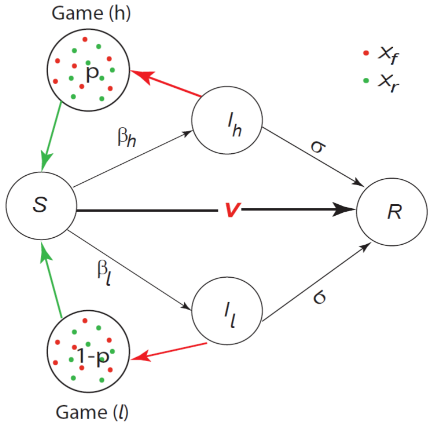

Fig. 1. The scheme of transition between groups S, I and R. The process is coupled with the evolutionary game between the proportions of Warned-Fake (x_f) and Warned-Real (x_r) individuals for each case of initial infection rates, i.e. high (h) and low (l)

In our quest to solve the model, we define the payoff matrix $A(I_\phi)$ as a function of the expected fraction of infected subgroup in the evolutionary game, embedding information about the state of the population as follows,

$$A(I_\phi) = I_\phi \begin{pmatrix} c_1 & k_f \\ k_r & c_2 \end{pmatrix} + (1 - I_\phi) \begin{pmatrix} \overline{c}_1 & \overline{k}_f \\ \overline{k}_r & \overline{c}_2 \end{pmatrix}, \qquad (2)$$

where c_1 and c_2 are the costs of curing an infected individual belonging to any group, while $\overline{c}_1$ and $\overline{c}_2$ represent the cost of preventive measures before the agent reaches the condition of infection. Furthermore, we assume that prevention is less costly than treatment, so that ($c_i >> \overline{c}_i$), with $i \in \{f, r\}$. This assumption is not unrealistic, given that the government aims at reducing the number of infected individuals to a minimum, in order to flatten the infection curve. During the evolutionary game, individuals do not alter their beliefs when interacting with like-minded people. However, when Warned-Fake interact with Warned-Real, there may be a transition from one group to the other for each of them. We denote by $(1 - \mu)$ the probability of transitioning from Warned-Fake to Warned-Real, while $(1 - \nu)$ is the probability of the opposite direction. We then provide explicit form of the cost parameters $k_i >> \overline{k}_i$, with $i \in \{f, r\}$ as follows,

$$\begin{aligned} k_f &= c_1\mu + c_2(1-\mu), & k_r &= c_2\nu + c_1(1-\nu), \\ \overline{k}_f &= \overline{c}_1\mu + \overline{c}_2(1-\mu), & \overline{k}_r &= \overline{c}_2\nu + \overline{c}_1(1-\nu). \end{aligned} \qquad (3)$$

The dynamic evolutionary equations for the fractions of Warned-Fake x_f and Warned-Real x_r are given by

$$\begin{aligned} \dot{x_f}(t) &= (p(e_f, X) - p(X, X))x_f(t), \\ \dot{x_r}(t) &= (p(e_r, X) - p(X, X))x_r(t), \end{aligned} \qquad (4)$$

where $X(t) = (x_f(t), x_r(t))$, $x_f(t) = 1 - x_r(t)$, $e_f = (1, 0)$, $e_r = (0, 1)$ denote pure strategies, and $p(\cdot, \cdot)$ is the payoff function. We shall also assume that in the evolutionary game we are considering symmetric games and therefore the payoff matrix of the second player is $B = A(I_\phi)^T$. The expected payoff of the i-th strategy of the first player is given by

$$p(e_f, X) = e_f A(I_\phi)X,\ p(e_r, X) = e_r A(I_\phi)X. \qquad (5)$$

Evolutionary dynamics [19] for extended payoff matrix (2) is given by

$$\dot{x}_f(t) = x_f x_r Q(x_f, x_r, I_\phi), \qquad (6)$$

where $Q(x_f, x_r, I_\phi) = p(e_f, X) - p(e_r, X)$.

Simplified substitutions and calculations lead to the following differential equation describing the evolution of the proportion of informed-fake individuals.

$$\dot{x}_f = x_f^2 x_r(\overline{c}_1 - \overline{k}_r + I_\phi(c_1 - \overline{c}_1 - k_r + \overline{k}_r)) + x_f x_r^2(\overline{k}_f - \overline{c}_2 + I_\phi(k_f - \overline{k}_f - c_2 + \overline{c}_2)). \quad (7)$$

2. Hidden Control Approach

In this section, we introduce the control parameters. Recall that the regulator's objective is to boost the share of followers of real news by encouraging the dissemination of real information and restraining the spread of fake news. This approach is referred to as *Hidden Control*. We define the control parameters $u_i(t)$, $i = \{1, 2\}$, as the investment strategies that will contribute to improving the gain components for real news in the gain matrix

$$A(I_\phi) = I_\phi \begin{pmatrix} c_1 & k_f \\ k_r & c_2 + u_1 \end{pmatrix} + (1 - I_\phi) \begin{pmatrix} \overline{c}_1 & \overline{k}_f \\ \overline{k}_r & \overline{c}_2 + u_2 \end{pmatrix}. \quad (8)$$

We assume that exposure to real information, e.g. advertising campaigns, awareness campaigns, monetary incentives, contributes to the likelihood of having a favorable attitude towards a preventive behavior, in our scenario we consider the example of immunization by vaccination. To reflect this, we introduce the parameter $v(t) \in [0, 1]$ as the proportion of the susceptible subgroup that accepts early vaccination. For instance, whenever $v(t) = 0,5$, half of all susceptible individuals are inoculated. On the other hand, if $v(t) = 0$, everyone is vaccine-free, and if $v(t) = 1$, the susceptible subgroup as a whole is immunized. The dynamics of the system given in (9) becomes,

$$\begin{array}{l} \dot{S}_\phi = -\beta_\phi S_\phi I_\phi - v S_\phi x_r, \\ \dot{I}_\phi = \beta_\phi S_\phi I_\phi - \sigma I_\phi, \\ \dot{R}_\phi = \sigma I_\phi + v S_\phi x_r, \\ \dot{x}_f = x_f x_r Q(x_f, x_r, I_\phi). \end{array} \quad (9)$$

Next, we introduce and discuss the optimal control structure as a function of the concavity (convexity) characteristics of the cost functions.

2.1. Optimal Control Structure

As one might expect, the implementation of the hidden control approach doesn't come without cost to the government. We define J as the objective function that groups the cost functions in our model, i.e. the cost of infections $f(I_\phi(t))$, the cost of raising public awareness $h_i(u_i(t))$, and the vaccination cost $l(v(t))$. $f(I_\phi(t))$ is assumed to be non-decreasing, twice-differentiable and convex, with $f(0) = 0$, $f(I_\phi) > 0$ for all $I_\phi(t) > 0$. $h_i(u_i(t))$ and $l(v)$ are twice-differentiable and increasing functions in $u_i(t)$ and $v(t)$ such that $h_i(0) = 0$, $h_i(x) > 0$, $i = 1, 2$ when $x > 0$ (the same characteristics are retained for the $l(\cdot)$ functions).

The aggregated system costs over the time interval $[0, T]$ are then defined as

$$J = \int_0^T \Big(f(I_\phi(t)) + h_1(u_1(t)) + h_2(u_2(t)) + l(v(t)) \Big) dt. \quad (10)$$

The regulator is then faced with an optimal control problem in which these costs must be minimized, i.e. $\min_{\{u_1, u_2, v\}} J$.

Using Pontryagin's maximum principle, we build the optimal control $u_1(t), u_2(t), v(t)$ to the minimisation problem [20]. Next, we define the associated Hamiltonian H and adjoint functions $\lambda_{S_\phi}(t)$, $\lambda_{I_\phi}(t)$, $\lambda_{R_\phi}(t)$, $\lambda_{x_f}(t)$, $\lambda_{x_r}(t)$ and as follows

$$H = -J + \textstyle\sum_X \lambda_i \dot{b}, \quad \dot{\lambda}_X = -\frac{H}{X}, \text{where } X = \{S_\phi, I_\phi, R_\phi, x_r, x_f\} \quad (11)$$

with the following transversality conditions

$$\lambda_{S_\phi}(T) = \lambda_{I_\phi}(T) = \lambda_{R_\phi}(T) = \lambda_{x_f}(T) = \lambda_{x_r}(T) = 0. \quad (12)$$

According to Pontryagin's maximum principle, there exist continuous and piece-wise continuously differentiable co-state functions $\lambda(t) = (\lambda_{S_\phi}(t), \lambda_{I_\phi}(t), \lambda_{R_\phi}(t), \lambda_{x_f}(t), \lambda_{x_r}(t))$ that satisfy (11) and (12) for $t \in [0, T]$ together with continuous functions $u_1^*(t)$, $u_2^*(t)$, and $v^*(t)$:

$$(u_1^*, u_2^*, v^*) \in \arg\max_{u_1,u_2,v} H(\lambda, S_\phi, I_\phi, R_\phi, x_f, x_r, u_1, u_2, v). \tag{13}$$

Proposition 1. *The following statements apply to the optimal control problem described in this section:*

- *When $h_i(\cdot)$ are concave functions, then there exists $t_0 \in [0, T]$ such that for $i = 1, 2$:*

$$u_i^*(t) = \begin{cases} u_i^{max}, & \text{for } 0 \le t \le t_0; \\ 0, & \text{for } t_0 < t \le T. \end{cases}$$

- *When $h_i(\cdot)$ are strictly convex functions, then there exist the time t_0, t_1, $0 < t_0 < t_1 < T$ such that for $i = 1, 2$ ($\alpha(t) \in (0, u_i^{max})$):*

$$u_i^*(t) = \begin{cases} u_i^{max}, & \text{for } 0 \le t \le t_0; \\ \alpha(t), & \text{for } t_0 < t \le t_1; \\ 0, & \text{for } t_1 < t \le T. \end{cases}$$

Same proposition holds for vaccination parameter $v(t)$. We define functions $\psi_i(t)$ as follows:

$$\begin{aligned} &\psi_1(t) = (\lambda_{x_r}(t) - \lambda_{x_f}(t))x_f(t)x_r^2 I_\phi(t), \\ &\psi_2(t) = (\lambda_{x_r}(t) - \lambda_{x_f}(t))x_f(t)x_r^2(1 - I_\phi(t)), \\ &\psi_3(t) = (\lambda_{R_\phi}(t) - \lambda_{S_\phi}(t))S_\phi(t)x_r. \end{aligned} \tag{14}$$

Proposition 2. *Functions $\psi_i(t)$, $i = \overline{1,3}$ are decreasing functions of $t \in [0, T]$.*

Based on previous research [21], in this subsection we define the structure of the optimal control. Under the condition that $h_i(u_i)$ and $l(v)$ are increasing functions with respect to $I_\phi \ge 0$ and $S_\phi \ge 0$, the Hamiltonian then reaches its maximum if $\psi_i = \dot{h}_i(u_i) \ge 0$, $i = 1, 2$, and $\psi_3 = \dot{l}(v) \ge 0$. We can find such u_i and v if and only if the following conditions are satisfied: $(\lambda_{x_r}(t) - \lambda_{x_f}(t)) \ge 0$ and $\lambda_{R_\phi}(t) - \lambda_{S_\phi}(t) \ge 0$.

2.2. Functions $h_i(\cdot)$ are Concave

In this subsection, we assume that $h_i(\cdot)$ is a concave function ($h_i''(\cdot) \le 0$), then, based on results in (11), the Hamiltonian is a convex function of $u_i(\cdot)$, $i = 1, 2$ and $v(\cdot)$. There are two different options for $u_i \in [0, u_i^{max}]$ and $v \in [0, v^{max}]$ that maximimize the Hamiltonian. If $-h_i(0) + \psi_i(t) \cdot 0 > -h_i(u_i^{max}) + \psi_i(t) \cdot u_i^{max}$ or $h_i(u_i^{max}) > \psi_i(t)u_i^{max}$, then the optimal control is $u_i = 0$; otherwise $u_i = u_i^{max}$. Same for the control parameter $v(t)$. For $i = \overline{1,2}$, the optimal control parameters $u_i(t)$ and $v(t)$ are defined as follows (same for the vaccination control $v^*(t)$):

$$u_i^*(t) = \begin{cases} 0, & \text{for } \psi_i(t)u_i^{max} < h_i(u_i^{max}), \\ u_i^{max}, & \text{for } \psi_i(t)u_i^{max} \ge h_i(u_i^{max}). \end{cases} \tag{15}$$

2.3. Functions $h_i(\cdot)$ are Strictly Convex

Here, we let $h_i(\cdot)$ to be a strictly convex function ($h_i''(\cdot) > 0$); so the Hamiltonian can be a concave function. Next, we assume the following derivative:

$$\frac{\partial}{\partial x}(-h_i(x) + \psi_i(t)x) \mid_{x=x_i} = 0. \tag{16}$$

There are three possible maxima for the Hamiltonian. This is a direct result to the fact that $x \in [0, u_i^{max}]$ and $u_i^*(t) = x_i$. Characterizing these three values requires solving the following derivatives of the Hamiltonian at $u_i = 0$ and $u_i = u_i^{max}$. If the derivatives (16) at $u_i = 0$ are non-increasing ($-h_i'(0)+\psi_i(t) \le 0$), then the value of the control that maximizes the Hamiltonian is less than 0, and according to our restrictions ($u_i \in [0, u_i^{max}]$) the optimal control will be equal to 0. If the derivatives at $u_i = u_i^{max}$ are increasing ($-h_i'(u_i^{max}) + \psi_i(t) > 0$), this means that the value of the control that maximizes the Hamiltonian is greater than u_i^{max}. Hence, the optimal control will be 1; otherwise, we can find the value of $u_i^* \in (0, u_i^{max})$ (same for the vaccination control $v^*(t)$):

$$u_i^*(t) = \begin{cases} 0, & \text{for } \psi_i(t) \le h_i'(0), \\ h'^{-1}(\psi_i(t)), & \text{for } h_i'(0) < \psi_i(t) \le h_i'(u_i^{max}), \\ u_i^{max}, & \text{for } h_i'(u_i^{max}) < \psi_i(t),\ i = 1, 2. \end{cases} \tag{17}$$

3. Direct Control Approach

Similarly, we provide the solution to optimal control in the direct control approach. Here, public awareness is raised by directly reducing the proportion of people exposed to “fake news”. the system dynamic is now given by

$$\begin{aligned} \dot{S}_\phi &= -\beta_\phi S_\phi I_\phi - v S_\phi x_r, \\ \dot{I}_\phi &= \beta_\phi S_\phi I_\phi - \sigma I_\phi, \\ \dot{R}_\phi &= \sigma I_\phi + v S_\phi x_r, \\ \dot{x}_f &= x_f x_r Q - u x_f. \end{aligned} \tag{18}$$

The definition of the cost functions are similar to the previous section. Aggregated system costs are given by,

$$J = \int_0^T \Big(f(I_\phi(t)) + h(u(t)) + l(v(t)) \Big) dt. \tag{19}$$

We now define the functions $\psi_i,\ i = 1, 2$ as follows,

$$\psi_1(t) = (\lambda_{x_r}(t) - \lambda_{x_f}(t)) x_f(t), \quad \psi_2(t) = (\lambda_{R_\phi}(t) - \lambda_{S_\phi}(t)) x_r(t) S_\phi(t). \tag{20}$$

- When $h_i(\cdot)$ and $l(\cdot)$ are concave functions, the optimal control structure is

$$u^*(t) = \begin{cases} u^{max}, & \text{for } \psi_1(t) u^{max} \ge h(u^{max}); \\ 0, & \text{for } \psi_1(t) u^{max} < h(u^{max}). \end{cases}$$

- When $h(\cdot)$ are strictly convex functions, the optimal control structure is

$$u^*(t) = \begin{cases} u^{max}, & \text{for } h'(u^{max}) < \psi_1(t); \\ h'^{-1}(\psi_i(t)), & \text{for } h'(0) < \psi_1(t) \le h'(u^{max}); \\ 0, & \text{for } \psi_1(t) \le h'(0). \end{cases}$$

Analogously, the structure of the optimal control for parameter the $v(t)$ can be defined.

4. Stability Properties and Steady-States

Thus far, the focus of our optimal control analysis has been on the left side of Fig. 1, specifically the S_ϕ–I_ϕ dynamics and information-flow interactions via a limited-vaccination evolutionary game (allowing direct S_ϕ to R_ϕ transitions). However, the primary objective of the regulator is to achieve an outbreak of the infection, with the aim of moving individuals into the R state as quickly and extensively as possible, with the ideal scenario being a state of $R = 1$ ($S = I = 0$). This motivates a theoretical note on the steady-state levels of R_ϕ, intended to spur reflection on the broader role of the model.

The disease-free equilibrium of the system (9) is defined as follows: $E_1 = (S_\phi, I_\phi, R_\phi) = (1, 0, 0)$. Initially, all individuals are susceptible, with a single homogeneous information group

($x_r = x_f = 0$), since no information or infection has been introduced. Following the declaration of an infection ($I_\phi > 0$), the virus is known to spread freely, resulting in the following equation: (9):

$$-\beta_\phi S_\phi I_\phi - S_\phi x_r = 0, \quad \beta_\phi S_\phi I_\phi - \sigma I_\phi = 0, \tag{21}$$

recall that $S_\phi + I_\phi + R_\phi = 1$, mainstream calculations lead to $R_0 = \dfrac{\beta_\phi}{\sigma}$. The new equilibrium associated with the outbreak then becomes $E_2 = (\frac{1}{R_0}, 0, 1 - \frac{1}{R_0})$ [22].

Now, the information stream can be introduced into the game and the evolutionary game starts and is given by the following equation,

$$\dot{x}_f = x_f x_r Q(x_f, x_r, I_\phi).$$

We note that four equilibria (fixed points) can be drawn from the above function depending on the division of the players between Warned-Fake and Warned-Real groups such as $(0,0), (1,0), (0,1), (\widehat{x}_f, 1 - \widehat{x}_f)$, where

$$\widehat{x}_f = \frac{\bar{c}_2 - k_f + I_\phi(c_2 - \bar{c}_2 - k_f - \bar{k}_f)}{\bar{c}_2 - c_2 - \bar{k}_r - \bar{k}_f + I_\phi(c_1 - \bar{c}_1 - k_r - \bar{k}_r - k_f - \bar{k}_f + c_2 + \bar{c}_2)}.$$

Solving for the final state of the epidemic size we obtain,

$$\frac{dS_\phi}{dR_\phi} = -R_0 S_\phi. \tag{22}$$

And the steady-state for the susceptible subgroup is then derived such that,

$$S_\phi(\infty) = S_\phi(0) e^{-R_0[R_\phi(\infty) - R_\phi(0)]}$$

based on the fact that the ultimate solution would sustain a zero infection rate, i.e. $I_\phi(t) = 0$, and since $S_\phi(\infty) = 1 - R_\phi(\infty)$ we then have the recovered steady-state value corresponding to the final epidemic size as follows (With $R_0 > 1$ implies $R_\phi(\infty) > 0$):

$$R_\phi(\infty) = 1 - e^{-R_0(R_\phi(\infty))}.$$

5. Numerical Simulation

To illustrate our theoretical results, we perform a series of numerical calculations in the form of experiments [23]. The constellation of parameter values remains unchanged for all our experiments, such that, $\beta_l = 0,1$; $\beta_h = 0,3$; $\sigma = 0,05$; $I_l = 0,05$; $I_h = 0,3$; $S_\phi(0) = 1 - I(0)$; $R_\phi(0) = 0$; $x_f(0) = 0,9$; $x_r(0) = 0,1$. The costs are given by $f(I_\phi) = 50 I_\phi(t)$; $l(v(t)) = 5v(t)$; $v^{max} = 0,15$. Costs of raising public awareness are $h_1(u_1(t)) = 15u_1^2(t)$ and $h_2(u_2(t)) = 10u_2^2(t)$. The payoff matrix parameters are respectively given by $c_1 = -0,3$; $c_2 = -0,2$; $\overline{c}_1 = -0,2$; and $\overline{c}_2 = -0,1$. For each experiment, we run the model for the time interval $t \in [0, 100]$.

In combining every possible case arising from the realization of the probabilistic values of β_ϕ and I_ϕ, we are left with 36 cases. To alleviate the burden of the curse of dimensionality, we consider only two values of β_ϕ coupled with alternative cases. Realistically, a small value of β_ϕ corresponding to low virulence is likely to induce insignificant propagation of the virus within the population, yet this choice of case limitation allows us to answer our research question. Consequently, in order to test the model's sensitivity with regard to the probability parameter, we vary the parameter p in the stochastic interval $\{0, 0,2, 0,4, 0,6, 0,8, 1\}$.

Experiment 1. Hidden Control Approach & Low Infection Rate. This experiment shows the behaviour of the complex system if the control parameters are included into the structure of the payoff matrix. We show the case of low infection rate $\beta_l = 0,1$. Here, the control strategies ameliorate the value of an agent, which corresponds to capturing real news. We assume that reading real news assists in protecting the agents from mistakenly purchasing unnecessary or ineffective medicine for example. In Fig. 2 the behaviour of the SIR model and the evolutionary trends of the news dynamics are presented. Fig. 3 below shows the impact of the hidden control to the decisions of the population agents. The structure of the optimal control and aggregated costs is demonstrated in Fig. 2 and 3.

Given our set of constellation parameters considered for the payoff matrix, our model returns an aggregate cost value equivalent to $J_0 = 7,43 \cdot 10^7$ monetary units in the uncontrolled case and $J_1 = 2,95 \cdot 10^7$ monetary units in the controlled case. Hence, the application of the hidden control is an effective measure that protects the population from the consequences of epidemics.

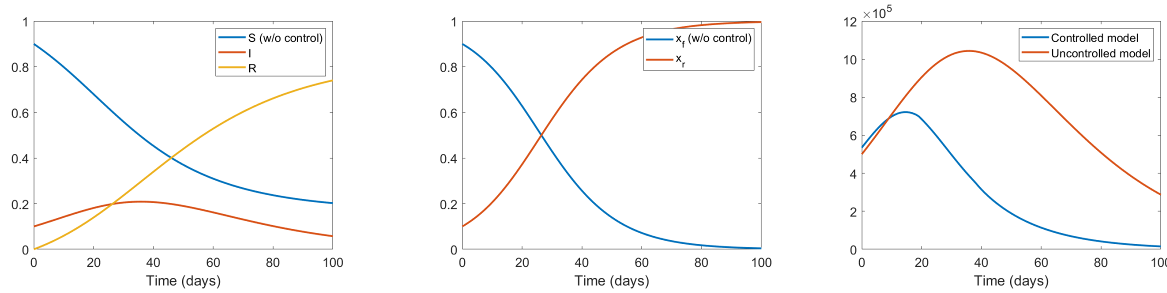

Fig. 2. SIR model (left) and evolution of the proportions fake x_f and real x_r news followers (middle) in uncontrolled case ($\beta_l = 0,1$). Comparison of the aggregated costs (right)

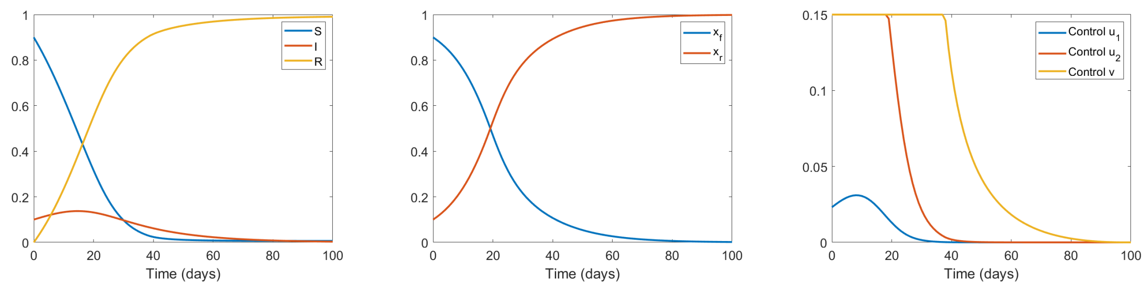

Fig. 3. SIR model (left) and evolution of the proportions fake x_f and real x_r news followers (middle) in controlled case ($\beta_l = 0,1$). Structure of the optimal control (right)

Experiment 2. Hidden control approach and High infection rate. Similarly, we draw conclusions for the case where hidden control is implemented when the expected infection rate is high. Aggregated costs are demonstrated in Fig. 4. Fig. 5 shows the impact of the hidden control to the decisions of the population agents and the structure of the optimal control.

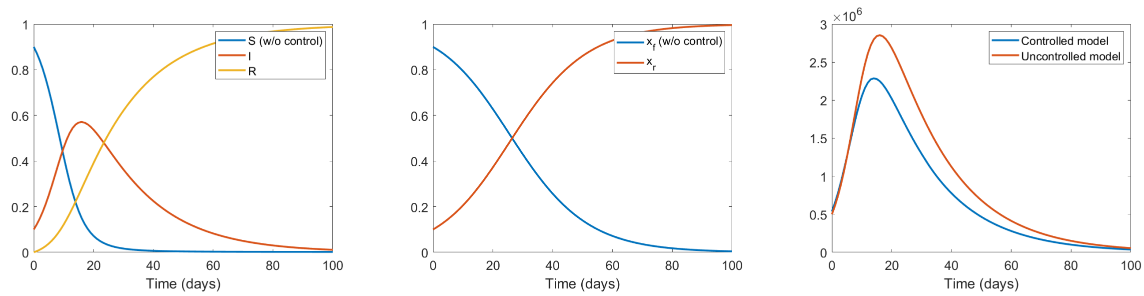

Fig. 4. SIR model (left) and evolution of the proportions fake x_f and real x_r news followers (middle) in uncontrolled case ($\beta_h = 0,3$). Comparison of the aggregated costs (right)

Given our set of constellation parameters considered for the payoff matrix, our model returns an aggregate cost value equivalent to $J_0 = 9,87 \cdot 10^7$ monetary units in the uncontrolled case and $J_1 = 7,6 \cdot 10^7$ monetary units in the controlled case. Once again, the application of the hidden control is revealed to be an effective measure.

In the next two experiments, we consider the second approach and assume that the impact of the control parameters is direct and convert individuals from the Warned-Fake to Warned-Real state.

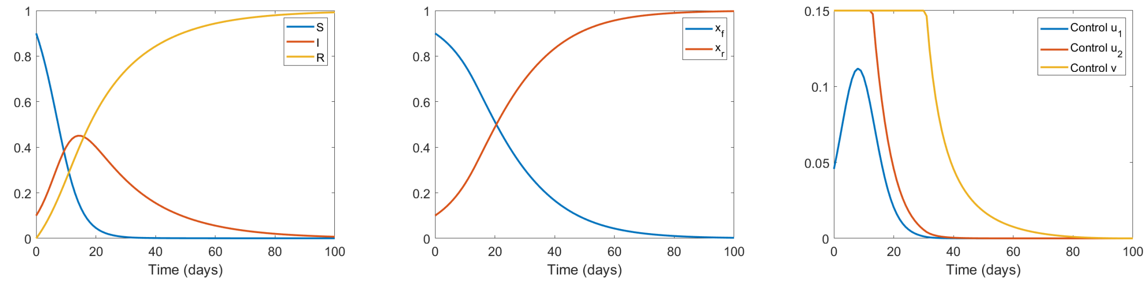

Fig. 5. SIR model (left) and evolution of the proportions fake x_f and real x_r news followers (middle) in controlled case ($\beta_h = 0,3$). Structure of the optimal control (right)

Experiment 3. Direct control approach and Low infection rate. Figs. 6, 7 depict the behaviour of the epidemic system and the evolutionary news dynamics in both uncontrolled and controlled cases respectively.

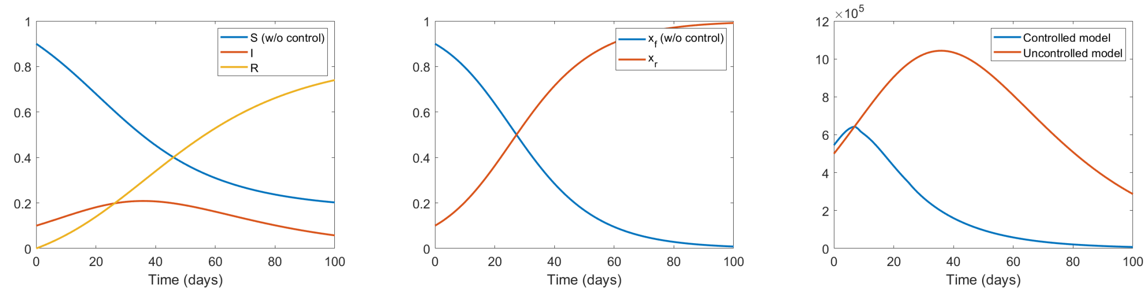

Fig. 6. SIR model (left) and evolution of the proportions fake x_f and real x_r news followers (middle) in uncontrolled case ($\beta_l = 0,1$). Comparison of the aggregated costs (right)

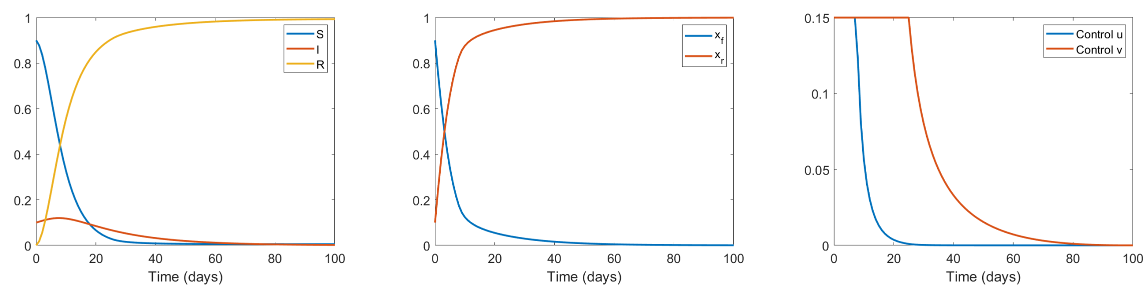

Fig. 7. SIR model (left) and evolution of the proportions fake x_f and real x_r news followers (middle) in controlled case ($\beta_l = 0,1$). Structure of the optimal control (right)

In the third experiment we get the following values of aggregated costs in the uncontrolled case $J_0 = 7,43 \cdot 10^7$ m. u. and $J_1 = 2,02 \cdot 10^7$ m.u. in the controlled case.

Experiment 4. Direct control approach & High infection rate. Figs. 8–9 depict the behaviour of the epidemic system and the evolutionary news dynamics in both uncontrolled and controlled cases respectively.

In the fourth experiment we get the following values of aggregated costs in the uncontrolled case $J_0 = 9,87 \cdot 10^7$ m. u. and $J_1 = 4,9 \cdot 10^7$ m.u. in the controlled case.

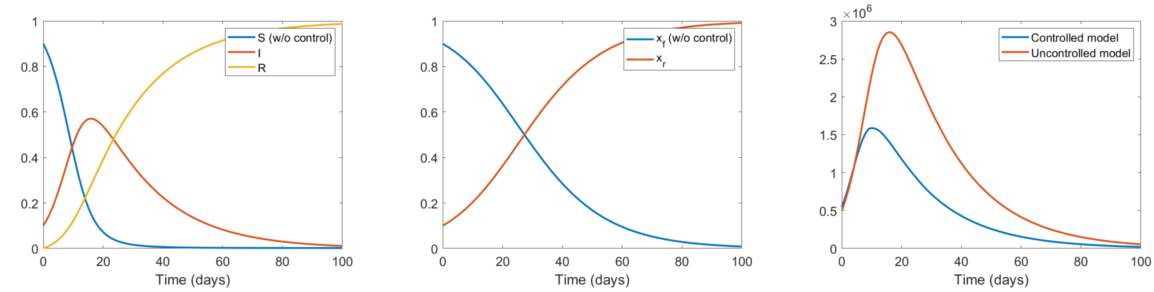

Fig. 8. SIR model (left) and evolution of the proportions fake x_f and real x_r news followers (middle) in uncontrolled case ($\beta_h = 0,3$). Comparison of the aggregated costs (right)

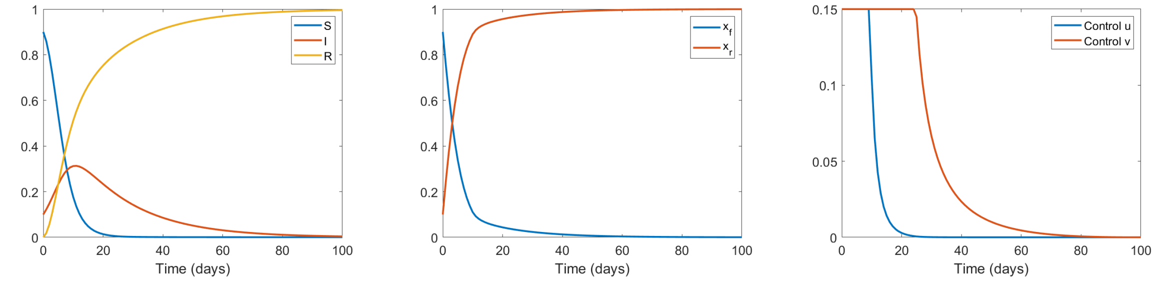

Fig. 9. SIR model (left) and evolution of the proportions fake x_f and real x_r news followers (middle) in controlled case ($\beta_h = 0,3$). Structure of the optimal control (right)

Concluding Remarks

We studied a stochastic evolutionary SIR model with interacting individuals whose infection dynamics are shaped by both social-planner interventions and information exchanges. Government investment in limiting fake news reduces the Warned-Fake population, while interactions between individuals exposed to different information types generate probabilistic transitions across information groups. This mechanism keeps evolutionary dynamics active by allowing individuals to revise or retain their beliefs.

Initial infection rates play a central role in the model and are treated here as exogenous. Yet, early pandemic decisions may themselves influence the speed of both viral and informational diffusion, while public panic can introduce additional noise into infection dynamics [24, 25]. Our numerical results contribute to debates on whether planners should disclose their actions and intentions when combating disease spread and misinformation. Direct control appears most effective, but it may also be perceived by individuals as intrusive or as limiting personal freedom.

Administrative and Legal Implications

Beyond its theoretical contribution, the model offers administrative and legal insights for early-stage pandemic management. First, its stochastic structure highlights the need for protocols that monitor uncertainty in infection indicators and information flows, including early-warning systems, coordination between epidemiological and communication units, and tracking of misinformation exposure. Second, the comparison between hidden and direct control shows that informational interventions depend on the regulatory framework governing public communication, including legal rules on awareness campaigns, misinformation control, and intervention in digital channels during health emergencies. Finally, the optimal-control results support adaptive administrative and legal mechanisms for allocating resources to awareness, testing, and immunisation under uncertainty. Thus, the model can inform both epidemiological strategies and institutional tools for early pandemic response.

Several extensions remain possible. Future work could introduce asymmetry between players, adopt richer epidemiological structures such as SIS or SIRS models to capture population subgroups, or model information diffusion through social networks where fake news spreads endogenously.

References

1. Capasso V. *Mathematical Structures of Epidemic Systems*. Heidelberg, Springer, 1993, 283 p. DOI: 10.1007/978-3-540-70514-7
2. Starnini M., Aleta A., Tizzoni M., Moreno Y. Impact of Data Accuracy on the Evaluation of COVID–19 Mitigation Policies. *Data & Policy*, 2021, vol. 3, no. e28, 10 p. DOI: 10.1017/dap.2021.25
3. Cramer E.Y., Yuxin Huang, Yijin Wang et al. The United States Covid-19 Forecast Hub Dataset. *Scientific Data*, 2022, vol. 9, article ID: 462, 15 p. DOI: 10.1038/s41597-022-01517-w
4. Hethcote H.W., Van Ark J.W. Epidemiological Models for Heterogeneous Populations: Proportionate Mixing, Parameter Estimation, and Immunization Programs. *Mathematical Biosciences*, 1987, vol. 84, no. 1, pp. 85–118. DOI: 10.1016/0025-5564(87)90044-7
5. Kermack W.O., McKendrick A.G. Contributions to the Mathematical Theory of Epidemics–I. 1927. *Bulletin of Mathematical Biology*, 1991, vol. 53, no. 1–2, pp. 33–55. DOI: 10.1007/BF02464423
6. Nowzari C., Preciado V.M., Pappas G.J.: Analysis and Control of Epidemics: A Survey of Spreading Processes on Complex Networks. *IEEE Control Systems Magazine*, 2016, vol. 36, no. 1, pp. 26–46. DOI: 10.1109/MCS.2015.2495000
7. Pastor-Satorras R., Castellano C., Mieghem V.M., Vespignani A. Epidemic Processes in Complex Networks. *Reviews of Modern Physics*, 2015, vol. 87, no. 3, pp. 925–979. DOI: 10.1103/RevModPhys.87.925
8. Gubar E., Taynitskiy V., Dahmouni I. The Impact of Fake News on Infection Dynamics in Pandemic Control: An Evolutionary SIR Model. *IFAC-PapersOnLine*, 2023, vol. 56, no. 2, pp. 1778–1783. DOI: 10.1016/j.ifacol.2023.10.1889
9. Paarporn K., Eksin C., Weitz J.S., Wardi Y. Optimal Control Policies for Evolutionary Dynamics with Environmental Feedback. *IEEE Conference on Decision and Control*, 2018, pp. 1905–1910. DOI: 10.1109/CDC.2018.8619604
10. Rocha Y. M., de Moura G.A., Desiderio G.A. et al. The Impact of Fake News on Social Media and Its Influence on Health During the COVID–19 Pandemic: A Systematic Review. *Journal of Public Health*, 2023, vol. 31, pp. 1007–1016. DOI: 10.1007/s10389-021-01658-z
11. Rowthorn R., Flavio T. The Optimal Control of Infectious Diseases Via Prevention and Treatment. *Technical Report 2013, Cambridge-INET Working Paper*, Cambridge, 2020, 57 p.
12. Modgil S., Singh R.K., Gupta S., Dennehy D. A Confirmation Bias View on Social Media Induced Polarisation During Covid–19. *Information Systems Frontiers*, 2021, vol. 26, pp. 417–441. DOI: 10.1007/s10796-021-10222-9
13. Khouzani M., Sarkar S, Altman E. Optimal Control of Epidemic Evolution. *Proceedings IEEE INFOCOM, Shanghai*, 2011, pp. 1683–1691. DOI: 10.1109/INFCOM.2011.5934963
14. Dahmouni I., Kuchesfehani E.K. Necessity of Social Distancing in Pandemic Control: A Dynamic Game Theory Approach. *Dynamic Games and Applications*, 2022, vol. 12, no. 1, pp. 237–257. DOI: 10.1007/s13235-021-00409-9
15. Gubar E., Policardo L., Sanchez Carrera E.J., Taynitskiy V. On Optimal Lockdown Policies While Facing Socioeconomic Costs. *Annals of Operations Research*, 2023, vol. 337, pp. 959–992. DOI: 10.1007/s10479-023-05454-8
16. Yunhan Huang, Quanyan Zhu. Game-Theoretic Frameworks for Epidemic Spreading and Human Decision-Making: A Review. *Dynamic Games and Applications*, 2022, vol. 12, no. 1, pp. 7–48. DOI: 10.1007/s13235-022-00428-0
17. Sethi S.P., Thompson G.L. *Optimal Control Theory: Applications to Management Science and Economics*. Springer, Berlin, 2005. DOI: 10.1007/0-387-29903-3
18. Taynitskiy V., Gubar E., Fedyanin D. et al. Optimal Control of Joint Multi-Virus Infection and Information Spreading. *IFAC-PapersOnLine*, 2020, vol. 53, no. 2, pp. 6650–6655. DOI: 10.1016/j.ifacol.2020.12.086
19. Weibull J.W. *Evolutionary Game Theory*. Cambridge, The MIT Press, 1995, 265 p.
20. Pontryagin L., Boltyanskii V., Gamkrelidze R., Mishchenko E. *The Mathematical Theory of Optimal Processes*. New York, Interscience Publishers, 1962.
21. Gubar E., Taynitskiy V., Quanyan Zhu. Optimal Control of Heterogeneous Mutating Viruses. *Games*, 2018, vol. 9, no. 4, 18 p. DOI: 10.3390/g9040103
22. Feng Fu, Rosenbloom D.I., Long Wang, Nowak M.A. Imitation Dynamics of Vaccination Behaviour on Social Networks. *Proceedings of the Royal Society B: Biological Sciences*, 2011, vol. 278, pp. 42–49. DOI: 10.1098/rspb.2010.1107
23. Sandholm W.H. *Population Games and Evolutionary Dynamics*. Cambridge, The MIT Press, 2010, 616 p.
24. Asadzadeh A., Samad-Soltani T., Rezaei-Hachesu P. Applications of Virtual and Augmented Reality in Infectious Disease Epidemics with a Focus on the COVID-19 Outbreak. *Informatics in Medicine Unlocked*, 2021, vol. 24, article ID: 100579, 8 p. DOI: 10.1016/j.imu.2021.100579
25. Erhu Du, Eddie Chen, Ji Liu, Chunmiao Zheng. How do Social Media and Individual Behaviors Affect Epidemic Transmission and Control? *Science of the Total Environment*, 2021, vol. 761, article ID: 144114, 10 p. DOI: 10.1016/j.scitotenv.2020.144114

Received February 12, 2026

УДК 517.977.52 **DOI: 10.14529/mmp260301**

СТОХАСТИЧЕСКАЯ ДИНАМИКА И ОПТИМАЛЬНОЕ УПРАВЛЕНИЕ В ЭПИДЕМИЧЕСКИХ МОДЕЛЯХ

***Е.А. Губар*[1]*, В.А. Тайницкий*[1]*, И. Дамуни*[2]**
[1]Санкт-Петербургский государственный университет, г. Санкт-Петербург, Российская Федерация
[2]Университет Британской Колумбии, г. Ванкувер, Канада

Мы разрабатываем эволюционную SIR-модель со стохастическим информационным слоем для анализа влияния неопределенности на динамику распространения инфекции на начальном этапе пандемии. Данный подход учитывает два вида неопределенности: (i) неопределенность в отношении показателей здоровья, включая неизвестные начальные темпы инфицирования, и (ii) неопределенность в процессе обновления информации, возникающую в результате взаимодействия индивидов, подверженных влиянию конкурирующих типов информации. Мы характеризуем свойства устойчивости стохастической системы и сравниваем полученную эволюционную динамику с динамикой соответствующей детерминированной модели. Затем мы формулируем и решаем сопутствующую задачу оптимального управления, определяя оптимальную траекторию информационного воздействия со стороны регулирующего органа. Результаты численного моделирования демонстрируют, как изменение параметров влияет на динамику инфекции и на оптимальный уровень вмешательства регулятора, направленного на повышение достоверности информации среди населения.

Ключевые слова: анализ системы управления; оптимальное управление; sir модель; эпидемический процесс; распространение дезинформации.

Елена Алексеевна Губар, доцент, Санкт-Петербургский государственный университет (г. Санкт-Петербург, Российская Федерация), e.gubar@spbu.ru.

Владислав Александрович Тайницкий, ассистент, Санкт-Петербургский государственный университет (г. Санкт-Петербург, Российская Федерация), tainitsky@gmail.com.

Ильясс Дамуни, профессор, Университет Британской Колумбии (г. Ванкувер, Канада), ilyass.dahmouni@ubc.ca.

Поступила в редакцию 12 февраля 2026 г.